

Development of Antibacterial Face Masks Utilizing Biologically Synthesized Zinc Sulfate Nanoparticles from *Bauhinia purpurea*

Balu Vinayagamurthy, and Palaniappan Seedevis*

Department of Medical Informatics, Saveetha School of Engineering, Saveetha Institute of Medical and Technical Sciences (SIMATS), Saveetha University, Chennai - 602105, Tamil Nadu, India

*Corresponding author: seedevisalem@gmail.com

Abstract

The aim of this study was to explore the development of antibacterial face masks utilizing biologically synthesized zinc sulfate nanoparticles sourced from the leaves of *Bauhinia purpurea*. The synthesized zinc sulfate nanoparticles were confirmed via UV-Vis spectral analysis, while their structural characteristics and morphology was examined through SEM and XRD analyses. The results confirmed the high stability and purity of the zinc nanoparticles. FTIR analysis verified the involvement of functional groups in the zinc nanoparticles. Furthermore, the antimicrobial efficacy of the produced zinc sulfate NPs was evaluated using the agar well diffusion process. The results demonstrated significant antibacterial efficacy, with maximum zone of inhibition sizes of 21 mm, 22 mm, 24 mm, and 23 mm observed against *S.aureus*, *E. faecalis*, *ps. aeruginosa*, and *E.coli*, respectively, at a concentration of 125µg/ml. Subsequently, nanoparticle-coated masks were found to exhibit antimicrobial effects, effectively inhibiting the growth of contaminated microorganisms. These findings highlight the potential of zinc nanoparticles derived from plant extracts to combat various pathogenic microorganisms. Thus, the synthesis of zinc nanoparticles was applied to coat masks, offering both safer breathing and protection against external microbes.

Keywords: Zinc nanoparticles; *B. purpurea*; Characterization; Antibacterial; Antibacterial Face Mask.

1. Introduction

Zinc nanoparticles have emerged as pivotal elements across scientific and

engineering landscapes, owing to their remarkable physical and chemical properties such as morphology, size, shape, and dispersibility. With diameters typically falling within the range of 1 to 100 nanometers, these nanoparticles exhibit distinctive characteristics compared to their bulk forms, primarily due to their high surface area to volume ratio and quantum size effects (1). Their versatility finds application in addressing a spectrum of global challenges including combatting infectious diseases, improving food and medicine, mitigating climate change impacts, advancing agricultural practices, and addressing environmental pollution (2).

The production of zinc nano-particles can be attained through diverse procedures including chemical reduction, sol-gel synthesis, and physical vapor deposition (3). Each technique offers precise control over the shape, size, and surface characteristics of the nanoparticles, facilitating tailored production for specific needs (4). The exceptional attributes of zinc nanoparticles stem from the inherent qualities of zinc as an element. Zinc is abundant, cost-effective, and environmentally benign, rendering it an excellent candidate for nanomaterial fabrication (5). Additionally, zinc exhibits high biocompatibility, low toxicity, and excellent stability, thereby enhancing its suitability for biomedical purposes such as drug delivery, imaging, and therapeutic interventions (6).

Incorporating biosynthesis methods utilizing plant extracts in an aqueous medium offers an affordable procedure. However, these approaches may face limitations in cases where hazardous compounds are present, leading to

the creation of harmful materials or disruption of the surface structure (7) (Li et al., 2011). The presence of such contaminants can result in environmental damage, emphasizing the importance of employing environmentally friendly methodologies in contemporary research. Furthermore, zinc oxide nanoparticles (ZnONPs) showcase a spectrum of advantageous properties, including antibacterial, antifungal, anti-diabetic, and larvicidal effects (8), rendering them invaluable in various bio-applications such as biosensing, drug distribution, gene transfer, and nanomedicine (9). So, the biological role of the nanoparticles based on the phytochemical constituents have been identified such as phenols, alkaloids, tannins, flavonoids, flavone and flavonone glycosides. It was derived in different parts of plant parts such as leaf, bark, and root (10 -11). They have been reported to own various advantageous properties including analgesic, anti-inflammatory, antipyretic, antidiabetic, antimalarial, antifungal, cytotoxic, free radical scavenging, and thyroid hormone-stimulating effects (12-14). Despite the recognized medicinal benefits of the plant's edible parts, there is a lack of published studies explicitly evaluating the polyphenolic content, antioxidant capacity, or antibacterial properties of its leaves. Therefore, this study aimed to investigate the development of antibacterial face masks using zinc sulfate nanoparticles biologically synthesized from *Bauhinia purpurea* leaves.

2. Material and Methods

2.1 Collection of plant leaves

The fresh leaves of *Bhahunia purpurea* were collected from the local area in and around of Salem Junction (Latitude 11.6703° N; Longitude 78.1133° E), Tamil Nadu, India. The collected leaves were cleaned with tap water followed by distilled water and shade dried. The dried leaves were powdered with help of mixer grinder

2.2 Preparation of aqueous plant leaf extract

25 g of leaf sample was boiled with 100 ml of distilled water at 60°C for 5 minutes

(15). And then the mixture was filtered using Whatman No. 1. filter paper. Then the extract was stored in a beaker tightly covered with aluminium foil and stored for further use at 40°C.

2.3 Preparation of zinc sulphate solution

The solution used in the synthesis of zinc sulphate nanoparticles was analytical grade. 3mM stock zinc sulphate in chloride free distilled water was prepared for 100ml using 0.1274g of zinc sulphate in a 250ml beaker. The beaker containing solution was tightly covered with non-absorbent cotton and kept away from direct light for further use.

2.4 Synthesis of zinc sulphate nanoparticles

The zinc sulphate nanoparticles were synthesized by pipetting out 90ml of ZnSO₄ solution in a clean and dry 250ml beaker and placed it on a magnetic stirrer and then slowly 10ml of prepared *Bhahunia purpurea* leaf extract was added. With the addition of extract, color of solution changes from bright green to dark brown. The solution was tightly covered and allowed for 24 hours at room temperature. Then the synthesized particles were recovered by keeping it hot air oven at 150°C for 3 days (16) (Fig. 1).

2.5 Characterization and structural morphology of zinc sulphate nanoparticle

To 1 ml of triple distilled water, 10 ml of silver nanoparticles (Ag NPs) synthesised via green synthesis (Ag NPs) of *Phyllanthus niruri* was added for recording intensity using



Fig. 1: Synthesis of zinc nanoparticle (A) Preparation of zinc sulphate chemical (B) Plant extract + zinc sulphate (C) Magnetic stirrer for 2 hours (D) Synthesis of zinc sulphate nanoparticle

UV-vis spectrophotometer (Shimadzu, Japan) at the series of 200 to 700 nm. The freeze-dried Ag using 20 kV Ultra high-resolution scanning electron microscope to learn its morphological and structural composition. On a carbon coated copper grid with size of mesh was 40×4 µm, thin films of Ag NPs were placed, with help of blotting paper and excessive solvent was cleared. In addition, the film was desiccated using a mercury lamp for 5 min. The surface of thin films of AgNPs was scanned. The functional group change on AgNPs surface was examined qualitatively involving FTIR spectroscopy Thermo scientific spectrum 6700 (Stuart, 2004). X- ray diffraction (XRD) pattern was attained utilizing X'Pert Pro X-ray diffractometer (Philip, Netherland) operated at a voltage of 40 kV and a 30-mA current with Cu Kα radiation in (2θ) configuration and zeta potential analysis (17).

2.6 Sample preparation for antibacterial activity

0.1 g of plant extract and Zinc sulphate Nano particle were mixed with 1ml of sterile distilled water and it was mixed well; this solution is used for antibacterial activity.

2.6.1 Antibacterial activity of zinc sulphate nanoparticle

The efficiency of the microbicidal activity of *Bhahunia purpurea* leaf extract and Zinc sulphate Nan particle was measured by agar well diffusion process against the following microorganism *Escherichia coli* (MTTC No:1698), *Bacillus subtilis* (MTTC No:1403), *Staphylococcus aureus* (MTTC No:3160) these cultures are swabbed on the nutrient agar medium using gel puncture well was created on the medium. 50µg/ml, 100µg/ml and 125µg/ml of Zinc sulphate nanoparticle are added to the respected well. Vancomycin disc used as a control. These plants were kept in an incubator at 37°C for 24 hours. The zone of inhibition was measured by millimetre (mm) (18).

2.7 Antioxidant activity

The DPPH test at 517 nm was used to assess the antioxidant activity of zinc

sulphate nanoparticles (ZnS NPs) from *B.purpurea*. The nanoparticles demonstrated considerable radical scavenging activity (RSA) throughout a concentration range of 200 to 1000 µg/mL, according to the data. When compared to common antioxidants like BHA and L-ascorbic acid, the antioxidant capacity of the *B. purpurea* ZnS NPs grew with concentration but stayed lower.

2.8 Antibacterial Face mask preparation using zinc sulphate nanoparticle

5g of zinc sulphate nanoparticle was taken in a Peaker and dissolved in 100ml of distilled mixed well in using of magnetic stirrer (500 rpm). Then, the cotton-based face mask was preferred and diffed into the zinc sulphate nanoparticle. The zinc sulphate nanoparticle coated face mask was fixed and remove the excessive moisture using Padding Mangle (Horizontal) (DL-2005H) for 3 times. Then the zinc sulphate nanoparticle face mask was dried at room temperature.

2.9 Statistical Analysis

The data were calculated using the SPSS 16.0 version (Statistical software package) to find the mean, standard deviation (±SD), regression equation values.

3. Results and Discussion

3.1 Characterization of zinc sulphate nanoparticle

UV-analysis of zinc nanoparticle

The synthesized zinc sulphate nanoparticles from the leaf extract of *Bauhinia purpurea* showed (Fig. 2). UV-Visible spectroscopy observation of a color change in the fluid confirmed improved light absorption and a broader absorption range compared to conventional zinc nanoparticles. Recorded to Shimadzu et al., UV-vis spectrophotometer using green synthesis (Ag NPs) of *Phyllanthus niruri*. This enhancement in absorbance is due to the adsorption of naturally synthesized nanoparticles onto the zinc sulphate surface. The produced sample's absorption spectra is recorded between 252 nm. The UV-Vis measurements revealed a distinct peak suggests the ZnS nanoparticles

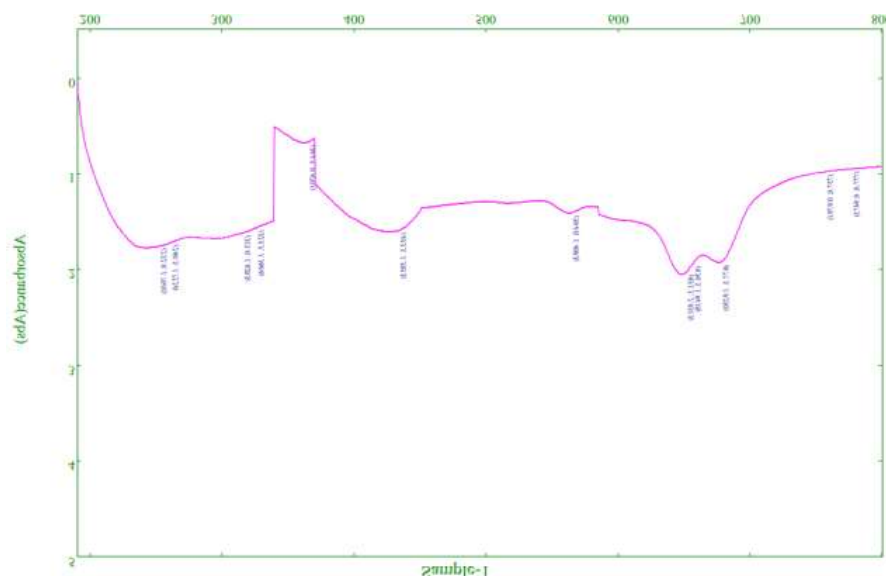


Fig. 2: UV-analysis of zinc nanoparticle

was synthesised using water extract from *B. purpurea* ZnS sulphate.

3.2 FT-IR analysis of zinc sulphate nanoparticle

The FT-IR analysis of zinc sulphate nanoparticles revealed the occurrence of 7 various functional groups, as summarized in (Fig. 3) the broad absorption range between 3327 cm^{-1} exhibited O-H stretching carboxylic acid, vibrations, while peaks at 2917 cm^{-1} and 2848 cm^{-1} C-H stretching were indicative alkane groups. The presence of a C=C stretching was confirmed by the peak observed at 1635 and 1538 cm^{-1} . Additionally, the spectrum displayed a peak at 1458 cm^{-1} corresponding to O-H carboxylic acid, and a peak at 406 cm^{-1} attributed to C-H vibrations of aromatic alcohols (Fig. 3). Remarkably, these findings closely align with earlier studies conducted by Mohan et al. (25), Kora et al. (26) and Shanmugam et al. (27).

XRD analysis of Zinc nanoparticle

XRD pattern of the synthesized zinc nanoparticle powder samples has exhibited a characteristic peak at 43 mins to 1 hr. The diffraction from distinct crystallographic

planes within the nanoparticles is represented in the peaks raised as it shows intensity peak at 11.730°C , 21.107°C , 23.300°C , 29.428°C , 34.190°C , 37.63°C , 42.130°C and 45.146°C which conforms the hexagonal crystalline structure depicted in (Fig. 4). Distinct peaks located at Bragg angles (2θ) = 34.190°C , 37.63°C , and 42.130°C (for zinc sulphate salt) when matched with JCPDS file 79.0208 for conformation from the obtained result are matching with the published articles. Similarly of XRD analysis was investigated *Pn*-AgNPs crystal structure agreement with earlier reported values (22, 23). The XRD report imitated that crystal assembly of all not produced trials are hexagonal wurtzite with an average crystallite size is about 25-27 nm conforming to inter-planar spacing, matrix constant and micro-strain of as produced powders (24).

SEM analysis of zinc nanoparticle

The Scanning Electron Microscope (SEM) analysis of the formulated zinc sulphate nanoparticle reveals uneven shape and rough surface roughness are seen in the (Fig. 5). In a prior report, propensity was recorded in many earlier outcome (19, 20).

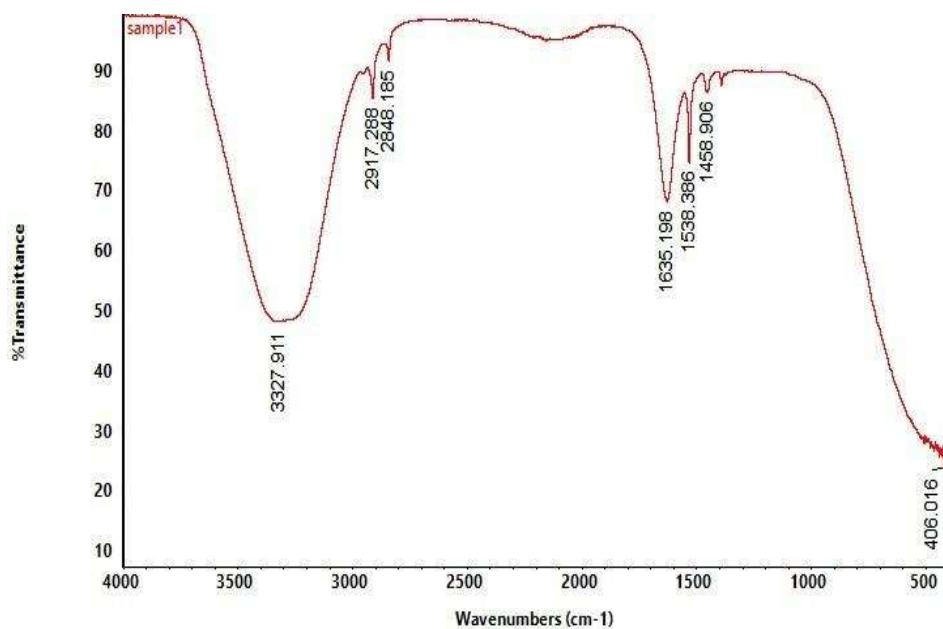


Fig. 3: FT-IR Analysis of zinc nanoparticle

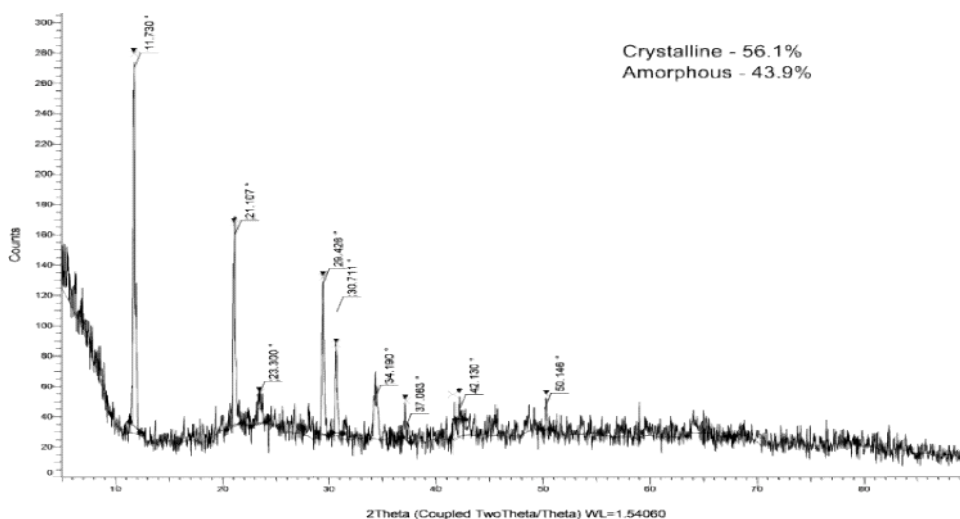


Fig. 4: XRD analysis of zinc nanoparticle

This result is in correspondences with a prior result, SEM noticed that the Ag NPs biosynthesized via the *H. auriculata* cake extract were mostly three-dimensional in shape (21.). The particles, which vary in size from nano to submicron, frequently group

together to create bigger aggregates. Their porous structure and large surface area imply increased reactivity, which makes them appropriate for a variety of industrial purposes including nanotechnology and agriculture fields.

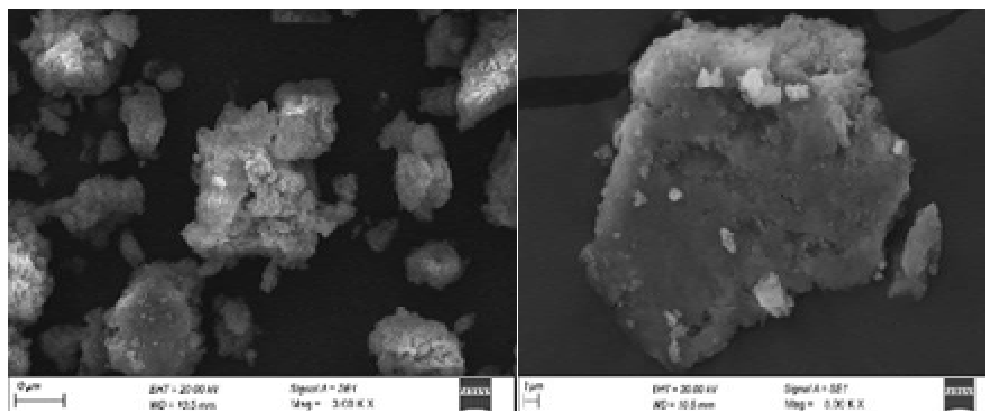


Fig. 5: (SEM) analysis of zinc nanoparticle

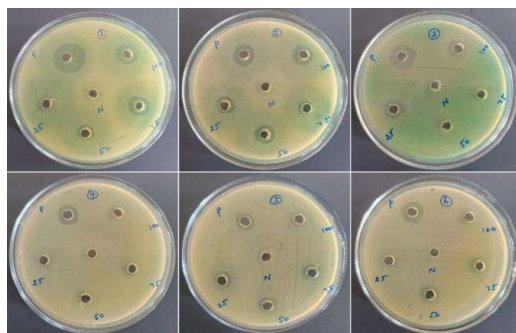


Fig 6: Antibacterial activity of ZnNPs

3.3 Antibacterial activity of zinc sulphate nanoparticle

The antibacterial activity of ZnNPs showed the zone of inhibition in all the four pathogens of *Staphylococcus aureus*, *Pseudomonas aeruginosa*, *Enterococcus faecalis*, and *Eschericia coli* (Figs. 6-8). The maximum inhibition zone 21, 22, 24 and 23 mm was recorded in 125µg/ml against *S. aureus*, *pseudomonas aeruginosa*, *E. faecalis*, and *E. coli*. The lowest inhibition was recorded 12 and 13 against *pseudomonas aeruginosa*, and *Eschericia coli* at 75 µg/ml concentration. The biocompatibility and antimicrobial properties of Phyllanthus niruri-AgNPs were evaluated against drug-resistant

human microbes including *S. aureus*, *E. coli*, *Pseudomona* spp., *P. vulgaris*, and *S. typhi* (28). Furthermore, AgNPs demonstrated their ability to inhibit pathogenic microorganisms such as *S. coccus* and *E. coli* (29). The antibacterial potential was evidenced by zones of inhibition tested against *S. aureus* (9.6 ± 0.58 mm) and *E. coli* (10.67 ± 0.58 mm) (30), while LEs exhibited modest antibacterial activity against *E. coli* and *S. aureus* with zones of inhibition measured at 3.67 ± 0.11 mm and 3.33 ± 0.13 mm respectively (31). Jiang et al. (32,33,34) argued that Zinc sulphate Nanoparticles have an efficient preference as anticancer and antimicrobial agents. Further, Zinc sulphate NPs have also been well defined for its bioavailability capacity of beneficial drugs or biomatter after working as drug shippers to achieve boosted treatment proficiency.

3.4 Antioxidant assay

ZnS NPs from *B.purpurea* is an antioxidant highly potential were tested to neutralize free radicals using the DPPH assay at concentrations ranging from 200 to 1000 µg/mL. The result was compared to reference antioxidants BHA and L-ascorbic acid (35). A dose-dependent increase in scavenging activity was demonstrated by the ZnS NPs.

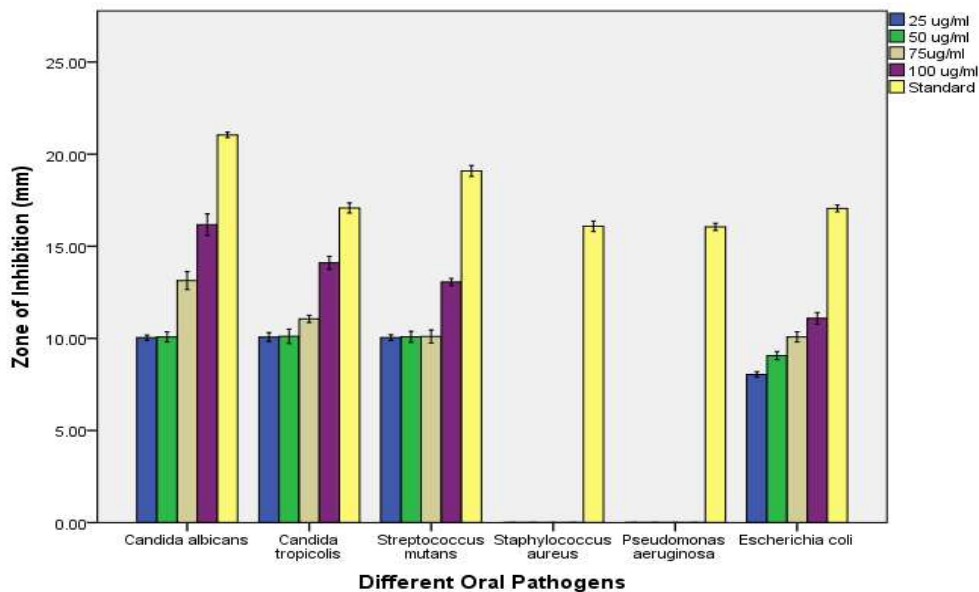


Fig. 7: Statistical Analysis of Antibacterial activity of ZnNPs

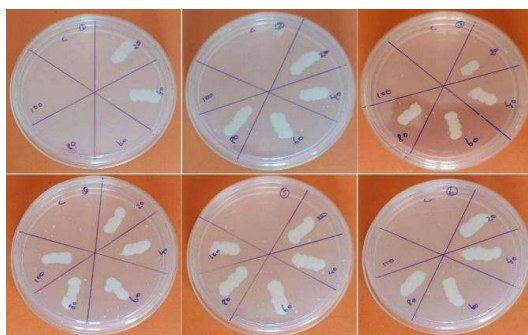


Fig. 8: Minimum bacterial concentration

The nanoparticles demonstrated values 20% inhibition at the minimum tested dosage of 200 µg/mL, typically highest response at the concentrations 55% at 1000 µg/mL. Despite this, BHA and L-ascorbic acid continued to exhibit much better antioxidant efficacy than ZnS NPs storing Antioxidant activity (36,37)

3.4 Antibacterial Face mask application using zinc sulphate nanoparticle

The synthesised Zinc sulphate Nps were fabricated in cotton cloth that stitched

into a mask to avoid air microbial contamination. Nanoparticle layered masks were exposed to antimicrobial outcome that serve to hinder the growth of contaminated microorganisms (Figs. 9-11). The minimum inhibitory concentrations of the nanoparticles against *E. coli*, *S. aureus*, *E. faecalis* and *Pseudomonas aeruginosa* respectively. The existence of an antimicrobial coating on cloth certainly suggests additional protection. Then its antibacterial activity was done to know the anti-microbial capacity of that particles. Zinc nanoparticles are capable of protecting our respiratory system without any entrance of unwanted microbes. So, the synthesized nanoparticle of zinc was coated on the mask to provide safest breath as well as from outside microbes.

Synthesized zinc sulphate nanoparticle mixed with water - (A), Cloth was dipped in beaker containing mixture of zinc sulphate nanoparticle - (B), Zinc sulphate nanoparticle coated with help of padding mangle machine -(C), Coated cloth was air dried- (D), control and zinc sulphate nanoparticle coated cloth – (E)

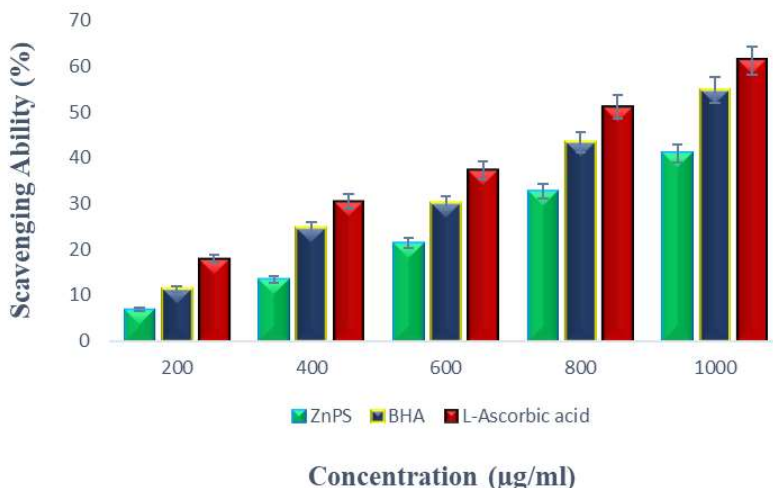


Fig. 9: Antioxidant assay

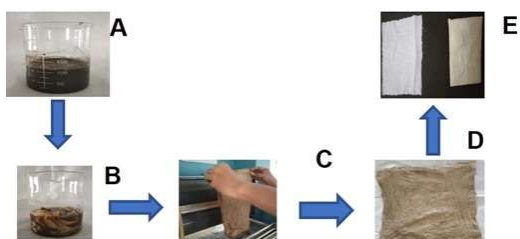


Fig. 10: Fabrication of *B. purpurea* ZnS NPs



Fig. 11: The Zinc sulphate NPs synthesized by using plant extract *Bauhinia purpurea* were coated on mask

4. Conclusion

In conclusion, the field of nanoscience and nanotechnology is advancing towards the development of eco-

friendly processes for synthesizing nanoparticles. In this study, zinc nanoparticles were successfully synthesized using *Bauhinia purpurea* leaf extract. Confirmation of zinc sulfate nanoparticles was achieved through UV-Vis spectral, SEM, and XRD analyses, which demonstrated high stability and absence of impurities. FT-IR analysis established the incidence of functional groups in the zinc sulfate nanoparticles. Moreover, the synthesized zinc sulfate nanoparticles exhibited significant antimicrobial activity. Application of these nanoparticles in coating masks resulted in effective inhibition of microbial growth, ensuring safer breathing and protection against external pathogens. The findings highlight the potential of zinc nanoparticles derived from plant extracts to combat various pathogenic microorganisms, further underscoring their utility in enhancing protective measures such as nanoparticle-coated masks.

References

1. Kumari, R., Sahai, A., & Goswami, N. (2015). Effect of nitrogen doping on structural and optical properties of Zinc sulphate nanoparticles. *Progress in Natural*

- Science: Materials International, 25(4), 300-309.
2. Agarwal, H., Kumar, S. V., & Rajesh kumar, S. (2017). A review on green synthesis of zinc sulphate nanoparticles—An eco-friendly approach. Resource Efficient Technologies. Karam, C., Habchi, R., Tingry, S., Miele, P., & Bechelany, M. (2018). Design of Multilayers of Urchin-like Zinc sulphate Nanowires Coated with TiO₂ Nanostructures for Dye-Sensitized Solar Cells. ACS Applied Nano Materials.
 3. Rochman, N. T., & Akwalia, P. R. (2017, May). Fabrication and characterization of Zinc sulphate (Zinc sulphate) nanoparticle by sol-gel method. In Journal of Physics: Conference Series (Vol. 853, No.1, p. 012041). IOP Publishing.
 4. Datta, A., Patra, C., Bharadwaj, H., Kaur, S., Dimri, N., & Khajuria, R. (2017). Green synthesis of Zinc sulphate Nanoparticles using parthenium hysterophorus leaf extract and evaluation of their antibacterial properties. Journal of Biotechnology and Biomaterials, 7, 271-275.
 5. Sutradhar, P., & Saha, M. (2016). Green synthesis of Zinc sulphate Nanoparticles using tomato (*Lycopersicon esculentum*) extract and its photovoltaic application. Journal of Experimental Nanoscience, 11(5), 314-327.
 6. Mohan, A. C., & Renjanadevi, B. (2016). Preparation of Zinc sulphate Nanoparticles and its characterization using scanning electron microscopy (SEM) and X-ray diffraction (XRD). Procedia Technology, 24, 761-766.
 7. McLaren, A., Valdes-Solis, T., Li, G., & Tsang, S. C. (2009). Shape and size effects of Zinc sulphate nanocrystals on photocatalytic activity. Journal of the American Chemical Society, 131(35), 12540-12541. 41
 8. Ahmed, S. A. (2017). Structural, optical, and magnetic properties of Mn-doped Zinc sulphate samples. Results in physics, 7, 604-610.
 9. Khalil, M. I., Al-Qunaibit, M. M., Al-Zahem, A. M., & Labis, J. P. (2014). Synthesis and characterization of Zinc sulphate nanoparticles by thermal decomposition of a curcumin zinc complex. Arabian Journal of Chemistry, 7(6), 1178-1184.
 10. Sutradhar, P., & Saha, M. (2015). Synthesis of Zinc sulphate Nanoparticles using tea leaf extract and its application for solar cell. Bulletin of Materials Science, 38(3), 653-657.
 11. Hasnidawani, J. N., Azlina, H. N., Norita, H., Bonnia, N. N., Ratim, S., & Ali, E. S. (2016). Synthesis of Zinc sulphate nanostructures using sol-gel method. Procedia Chemistry, 19, 211-216.
 12. Jiang, J., Pi, J., & Cai, J. (2018). The Advancing of Zinc sulphate Nanoparticles for Biomedical Applications. Bioinorganic chemistry and applications, 2018.
 13. Wang, Z. L. (2004). Zinc sulphate nanostructures: growth, properties and applications. Journal of physics: condensed matter, 16(25), R829.
 14. Matinise, N., Fuku, X. G., Kaviyarasu, K., Mayedwa, N., & Maaza, M. (2017). Zinc sulphate nanoparticles via *Moringa oleifera* green synthesis: physical properties & mechanism of formation. Applied Surface Science, 406, 339-347.
 15. Alenezi, M. R., Henley, S. J., Emerson, N. G., & Silva, S. R. P. (2014). From 1D and 2D Zinc sulphate nanostructures to 3D hierarchical structures with enhanced gas sensing properties. Nanoscale, 6(1), 235-247. 42
 16. Sindhura KS, Prasad TNVKV, Selvam PP, Hussain OM (2013) Synthesis, characterization and evaluation of effect of phytogenic zinc nanoparticles on soil exoenzymes. Appl Nanosci 1: 1-9.
 17. Alias, S. S., Ismail, A. B., & Mohamad, A. A. (2010). Effect of pH on Zinc sulphate nanoparticle properties synthesized by sol-gel centrifugation. Journal of Alloys and Compounds, 499(2), 231-237.
 18. Saundane, A. R., Vijaykumar, K., & Vajjinath, A. V. (2013). Synthesis of novel 2-amino-4-(5'-substituted 2'-phenyl-1H-indol-3'-yl)-6-aryl-4H-pyran-3-carbonitrile derivatives as antimicrobial and antioxidant agents. Bioorganic & medicinal chemistry letters, 23(7), 1978-1984.

19. Erdogan, O., Abbak, M., Demirbolat, G. M., Birtokocak, F., Aksel, M., Pasa, S., & Cevik, O. (2019). Green synthesis of silver nanoparticles via *Cynara scolymus* leaf extracts: The characterization, anticancer potential with photodynamic therapy in MCF7 cells. *PLoS one*, 14(6), e0216496.
20. Baranitharan, M., Kandeel, M., Shanmugavel, G., Kaliyaperumal, K., Subramanian, K., Elumalai, K., & Velmurugan, S. (2022). Fabrication of Silver Nanoparticles Using *Fimbristylis miliacea*: A Cheap and Effective Tool against Invasive Mosquito Vector, *Aedes albopictus*. *Journal of Nanomaterials*, 2022.
21. Benelli, G. (2016). Plant-mediated biosynthesis of nanoparticles as an emerging tool against mosquitoes of medical and veterinary importance: a review. *Parasitology research*, 115(1), 23-34.
22. Oves, M., Aslam, M., Rauf, M. A., Qayyum, S., Qari, H. A., Khan, M. S., ... & Ismail, I. M. (2018). Antimicrobial and anticancer activities of silver nanoparticles synthesized from the root hair extract of *Phoenix dactylifera*. *Materials Science and Engineering: C*, 89, 429-443.
23. Kavitha, S., Schikaran, M., Kannah, R. Y., Gunasekaran, M., Kumar, G., & Banu, J. R. (2019). Nanoparticle induced biological disintegration: a new phase separated pretreatment strategy on microalgal biomass for profitable biomethane recovery. *Bioresource technology*, 289, 121624.
24. Thaweesaeng, N., Supankit, S., Techidheera, W., & Pecharapa, W. (2013). Structure properties of as-synthesized Cu-doped ZnO nanopowder synthesized by co-precipitation method. *Energy Procedia*, 34, 682-688.
25. Mandal, V., Mohan, Y., & Hemalatha, S. J. P. R. (2007). Microwave assisted extraction—an innovative and promising extraction tool for medicinal plant research. *Pharmacognosy reviews*, 1(1), 7-18.
26. Kora, A. J., Sashidhar, R. B., & Arunachalam, J. (2010). Gum kondagogu (*Cochlospermum gossypium*): a template for the green synthesis and stabilization of silver nanoparticles with antibacterial application. *Carbohydrate Polymers*, 82(3), 670-679.
27. Shanmugam, S., & Gopal, B. (2014). Copper substituted hydroxyapatite and fluorapatite: Synthesis, characterization and antimicrobial properties. *Ceramics International*, 40(10), 15655-15662.
28. Kathireswari, P., Gomathi, S., & Saminathan, K. (2014). Plant leaf mediated synthesis of silver nanoparticles using *Phyllanthus niruri* and its antimicrobial activity against multi drug resistant human pathogens.
29. Pirtarighat, S., Ghannadnia, M., & Baghshahi, S. (2019). Green synthesis of silver nanoparticles using the plant extract of *Salvia spinosa* grown in vitro and their antibacterial activity assessment. *Journal of Nanostructure in Chemistry*, 9, 1-9.
30. Durian, G., Rahikainen, M., Alegre, S., Brosché, M., & Kangasjärvi, S. (2016). Protein phosphatase 2A in the regulatory network underlying biotic stress resistance in plants. *Frontiers in plant science*, 7, 194867.
31. Phetsouphanh, C., Darley, D. R., Wilson, D. B., Howe, A., Munier, C., Patel, S. K., & Matthews, G. V. (2022). Immunological dysfunction persists for 8 months following initial mild-to-moderate SARS-CoV-2 infection. *Nature immunology*, 23(2), 210-216.
32. Jiang, J., Pi, J., & Cai, J. (2018). The advancing of zinc oxide nanoparticles for biomedical applications. *Bioinorganic chemistry and applications*, 2018.
33. Srinivasan, P., Pitchai, A., & Ramasamy, P. (2025). Phosphorylated chitosan from the internal bone of *Sepia kobeensis* (Hoyle, 1885) and their inhibition against oral pathogens. *Carbohydrate Research*, 550, 109413.
34. Ali, B. S., Subhpradha, N., Pitchai, A., & Ramasamy, P. (2025). Harnessing Nanochitosan from *Sepia kobeensis* Cuttlebone for Cytotoxicity and Antimicrobial Applications in Dentistry: An In Vitro Study. *BioNanoScience*, 15(2), 218.
35. Das, B., Mounita, S., Ghosh, S., Khan, M. I., Indira, D., Jayabalan, R., & Balasubramanian, P. (2018). Biosynthesis of magnesium oxide (MgO) nanoflakes by using leaf extract of *Bauhinia purpurea* and

evaluation of its antibacterial property against *Staphylococcus aureus*. *Materials Science and Engineering: C*, 91, 436-444. howed around $72.22 \pm 0.22\%$ inhibition of DPPH.

36. Abbas Z, Irshad M, Ali S, Summer M, Rasheed A, Jawad M. Radical scavenging potential of spectrophotometric, spectroscopic, microscopic, and EDX observed zinc oxide nanoparticles from leaves, buds, and fowers extract of *Bauhinia*

variegata Linn: a thorough comparative insight. *Microsc Res Tech*. 2024;87(9):2121–33. <https://doi.org/10.1002/JEMT.24587>

37. Palaniappan, C. S., Pitchai, A., Duraisamy, R., Ganapathy, D., & Ramasamy, P. (2025). Synthesis, Characterization of Chitosan Nanoparticles from Cuttlebone of *Sepia prashadi* and Its Anticancer Efficacy Against MG63 Cell Line. *BioNanoScience*, 15(1), 209.